EE1L1 IP-1 Intermediate Project Report

Power amplifier

SubGroup A4-1

TU Delft

EE1L1 IP-1 Intermediate Project Report

Power amplifier

by

Sylke Misat
Boas op de Beek
Leon Abelmann
Ian van Ingen

EE1L1
20/12/2024

TU Delft

Contents

1

Introduction

This project focuses on the design, simulation, and analysis of a power amplifier using the LM3886TF operational amplifier.

The primary objective of the project is to design an amplifier circuit that meets the following requirements:
- Operates in a non-inverting configuration.
- Maintains a passband of 20 Hz to 40 kHz (-3 dB bandwidth), ensuring proper suppression of frequencies outside this range.
- Provides a voltage gain of 25 within the passband.
- Blocks any DC component from the input signal.

This report is organized as follows: Chapter 2 outlines the design methodology, including component selection and theoretical calculations. Chapter 3 presents the simulation results and analysis for frequency response and transient behavior. Chapter 4 shows the measurement results of the physical amplifier we built, and finally, in Chapter 5, our conclusions are presented.

2

Theory and Analysis (design methodology)

2.1. Circuit schematic

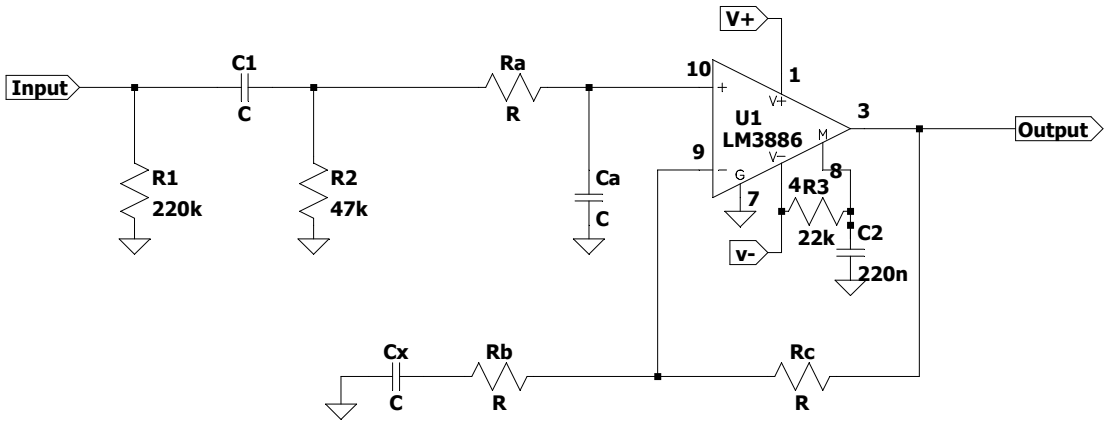

Figure 2.1: The power amplifier circuit

The entire circuit, as seen in Figure 2.1, may be divided into three different sub-circuits, namely the high-pass filter, low-pass filter, and the amplifier. The high-pass filter is responsible for the frequency cutoff at 20 Hz, whereas the low-pass filter takes care of the cutoff at 40.000 Hz. Lastly, the filters combined block out DC signals and the operational amplifier ensures a gain of 25.

2.1.1. High pass filter

The first part of the circuit can be interpreted as a high-pass filter, demonstrated in figure 2.2. After applying Kirchoff's current law (later referred to as KCL) at node B, we can obtain the following transfer function.

$$H(\omega) = \frac{v_o}{v_i} = \frac{j\omega C_1 R_2}{j\omega C_1 R_2 + 1} \tag{2.1}$$

The value of the capacitor must be chosen with the cutoff frequency of 20 Hz in mind. In order to calculate it we have used the following equations.

$$\omega = \frac{1}{R_2 C_1} \tag{2.2}$$

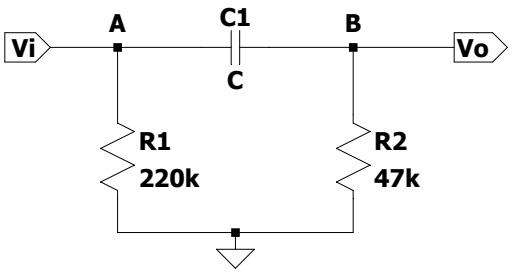

Figure 2.2: The high-pass filter

$$\omega = 2\pi \cdot f \tag{2.3}$$

After performing the calculations with R = 47.000 Ω, you are left with a capacitance of 169.3 nF.

2.1.2. Low pass filter

The second part of the circuit is the low-pass filter, as shown in Figure 2.3, which blocks all frequencies above 40.000 Hz.

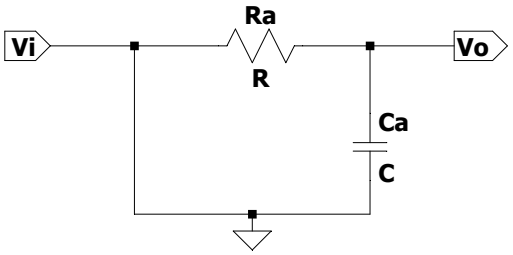

Figure 2.3: The low-pass filter

By applying KCL again, we get the following transfer function.

$$H(\omega) = \frac{v_o}{v_i} = \frac{1}{j\omega C_a R_a + 1} \tag{2.4}$$

[using Eqs. 2.4, 2.3 and some other as mentioned in the appendix, we get Ra = 3.6 kΩ and Ca = 1 nF] -> Lagers paper + calculations

2.1.3. Amplification

The final part of the circuit is the amplifier, which must have a gain of 25. Looking at figure 2.4, we can apply KCL in node A and obtain the following transfer function.

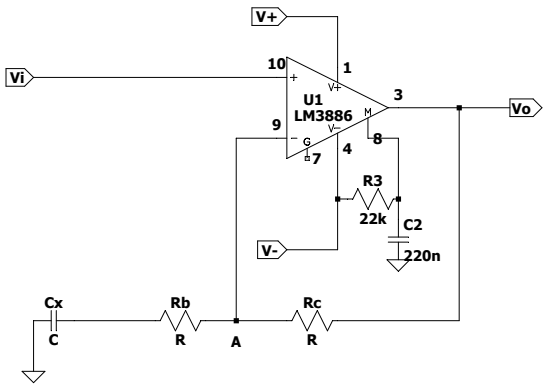

Figure 2.4: The amplification sub-circuit

$$H(\omega) = \frac{v_o}{v_i} = 1 + \frac{j\omega R_c C_x}{1 + j\omega R_b C_x} \tag{2.5}$$

By choosing Rc = 250 kΩ, Rb = 10 kΩ and Cx = 10uF we get a gain of 25.

2.2. Components and values

2.2.1. Unknown components

Since C1, R2, Ra and Ca are all part of the filter sub-circuit, we could not leave them out of the final build. And both Rb and Rc are needed for the gain, so therefore we will not be leaving any components out.

2.2.2. Component values

The lab only had limited components, so for clarity table 2.1 shows all of the ideal and matched values as well as the new calculations. All of the components that are not in this table we matched exactly.

Component	Ideal Value	Matched Value	New Calculation
C1	169 nF	150 nF	22.6 Hz
Ra	3.6 kΩ	3.9 kΩ	40809.0 Hz
Rc	25 kΩ	27 kΩ	$A = 27$

Table 2.1: Component values and calculations.

3

Simulation results

3.1. Frequency Response Simulation

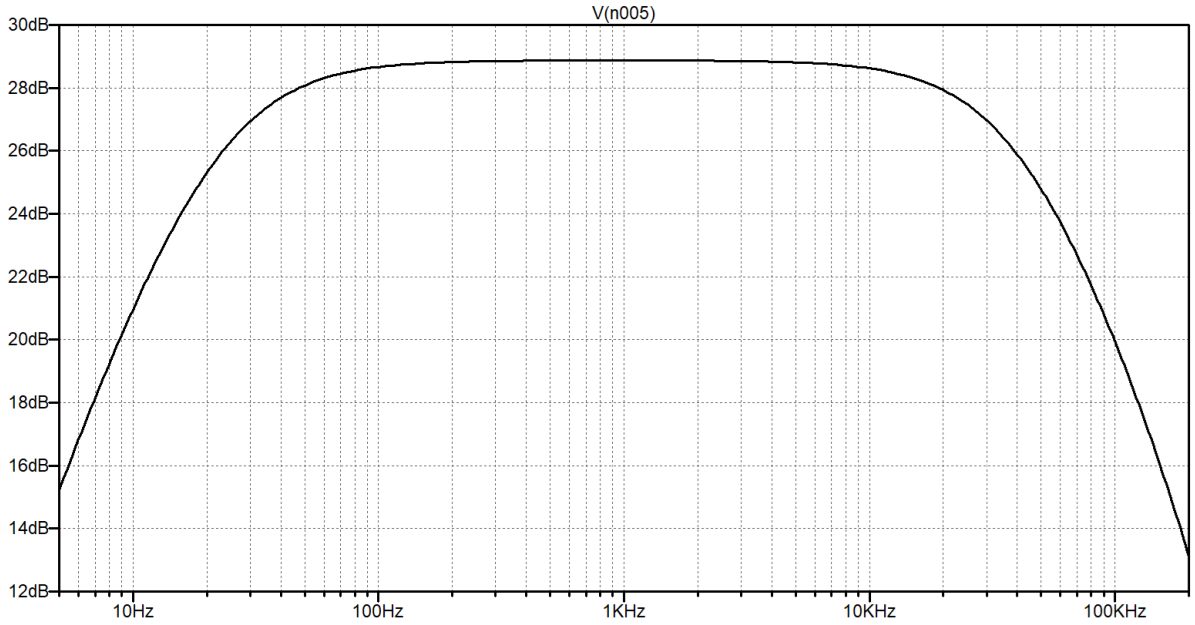

Figure 3.1: LTSpice simulation of the frequency response

The frequency response of the amplifier (fig. 3.1) was analyzed using AC simulation in LTspice to verify its gain characteristics and passband behavior. The simulation results show that the amplifier maintains a nearly constant gain of approximately +28.8dB within the passband range of 20 Hz to 40 kHz, corresponding to the expected voltage gain. At the lower cutoff frequency of 20 Hz and the upper cutoff frequency of 40 kHz, the gain drops by −3dB, reducing to approximately +25.8dB, which aligns with the -3 dB bandwidth requirement. Beyond the cutoff frequencies, the gain decreases steeply, demonstrating the filtering behavior of the circuit. This confirms that the designed amplifier successfully meets the specified passband and filtering criteria.

3.2. Transient Analysis

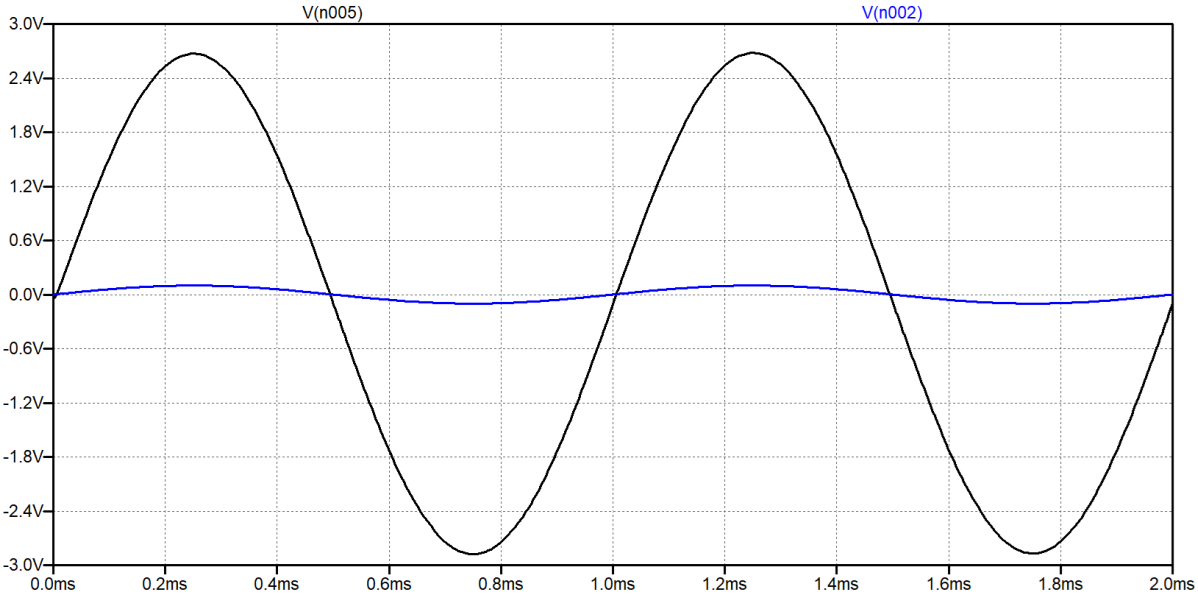

Figure 3.2: LTSpice simulation of the transient response

The transient response of the amplifier was simulated in LTspice to evaluate its time-domain performance and verify the gain and signal fidelity. A sinusoidal input signal with an amplitude of 0.1 V and a frequency of 1 kHz (within the passband) was applied, and the output signal was observed. The simulation results show a clean sinusoidal waveform at the output with an amplitude of 2.6 V, consistent with the calculated voltage gain. The output signal exhibits no noticeable distortion, and the phase shift between the input and output is minimal, as expected for frequencies within the passband. These results confirm that the amplifier accurately amplifies the input signal while maintaining signal integrity and adhering to the specified gain requirements.

4

Measurement results

After simulating the circuit, we built the amplifier and measured the gain using a function generator and oscilloscope.

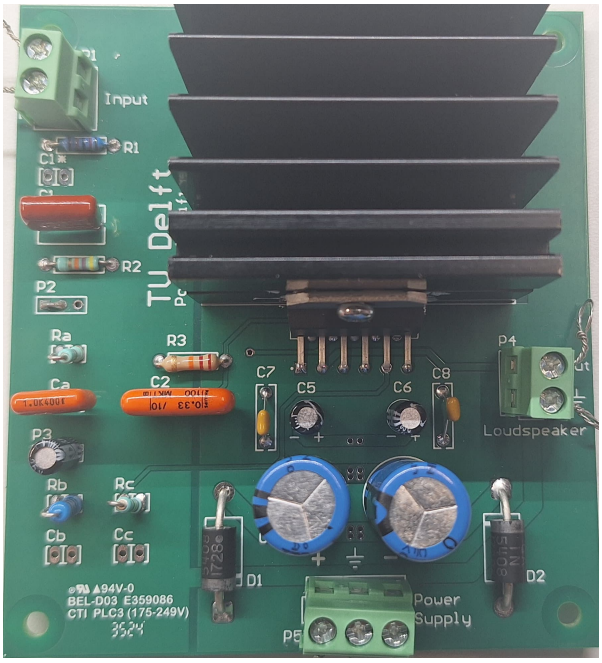

Figure 4.1: The assembled amplifier

4.1. Gain measurements

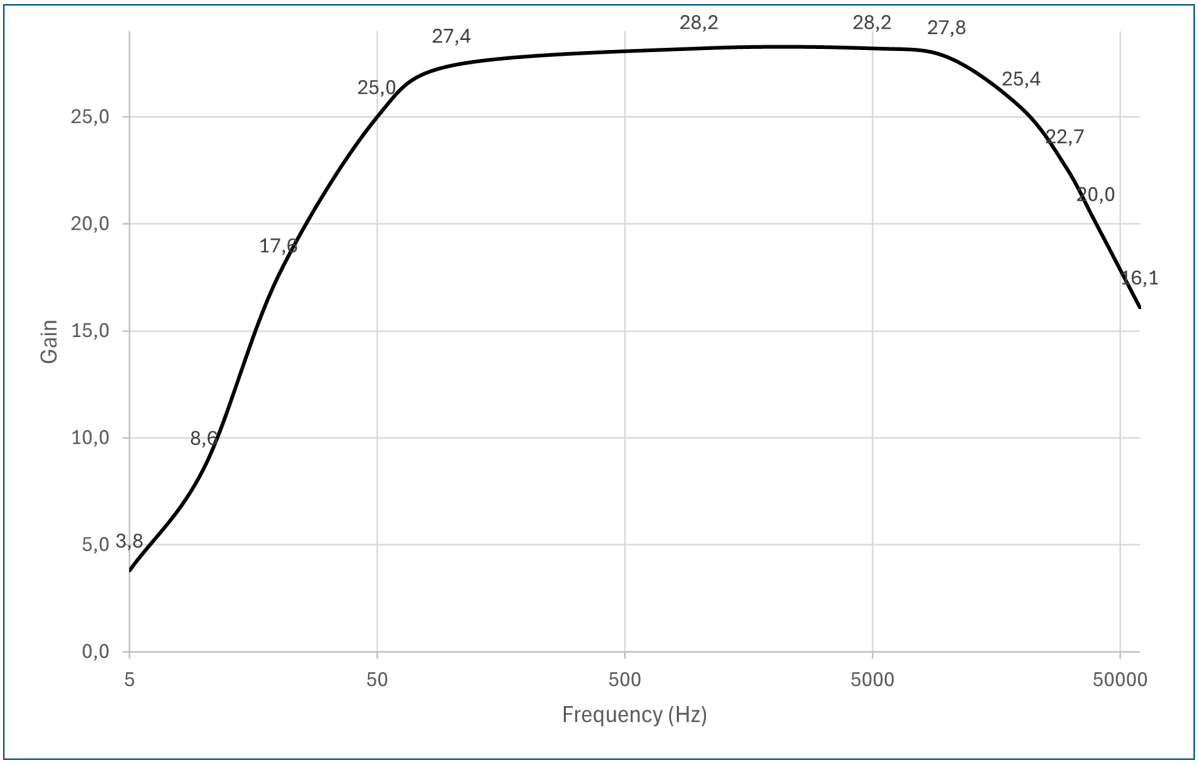

Figure 4.2: The frequency response of the amplifier, measured with an oscilloscope

The frequency response of the amplifier was experimentally measured using an oscilloscope to verify the gain and bandwidth characteristics. A sinusoidal input signal with a constant amplitude of 0.1 V was applied to the amplifier while its frequency was swept across a wide range, from below the lower cutoff, to beyond the upper cutoff. The input and output waveforms were observed on the oscilloscope, and the output amplitude was measured at various frequencies. Beyond the cutoff frequencies, the output amplitude decreased sharply, confirming the filtering behavior of the circuit. These measurements validated the simulation results and demonstrated the amplifier's compliance with the design specifications.

5

Conclusions

Based on all of the measurements our calculations were correct, but as mentioned in 2.2.2 we had to change a few values which made a difference most noticeable with the gain. Our cutoff frequencies are 23 Hz and 40809 Hz, we have a gain of 27 across the op amp and DC sources get blocked.

For future projects we would try to get closer to the ideal values of components.

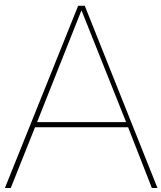

Appendix

Bandpass filter analysis

Ioan E. Lager

Experience shows that most groups opt for implementing their EPO-1 power amplifier [1, Section 18.3] by inserting a bandpass filter between the circuit's input and the opamp – the relevant bandpass filter and the correspondences with the notation in [1, Fig. 18.6] are given in Fig. 1. Students calculate the amplification of the opamp circuit by assuming a lossless (unit) transfer in the pass-band of this filter. However, it can be easily shown that the topology in Fig. 1 *does not yield a unit transfer*. Moreover, in view of R_1 having a *fixed* value $R_1 = 47\text{k}\Omega$ (this value is soldered on the provided PCB and may not be changed), the drop with respect to the unit transfer can be extremely significant and this *must* be accounted for in the choice for the R_2 resistance. Moreover, upon choosing R_2, the effectively obtained pass-band transfer must be accounted for determining the needed correction of the required amplification in the opamp circuit.

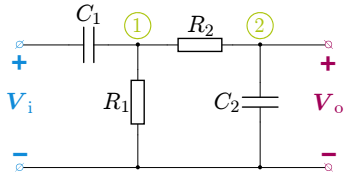

Figure 1: The analysed bandpass filter. The following correspondences between the hereby employed notations and those in [1, Fig. 18.6] apply: $R_1 \to R_2$, $R_2 \to R_\text{a}$, $C_2 \to C_\text{a}$ (the magenta symbols occur in [1, Fig. 18.6]). For avoiding ambiguities, this document will consistently make use of the notation in this figure, exclusively.

This document presents a detailed calculation of the transfer function $\boldsymbol{H}(f)$, with f denoting the frequency, that applies to the filter in Fig. 1. A parameter analysis illustrating the impact of R_2 on the entailed transfer will also be given. The document focuses on $|\boldsymbol{H}(f)|$. However, the derived expression of $\boldsymbol{H}(f)$ can be straightforwardly used for inferring the phase characteristic, as well. This study is supplemented with an analysis of the input impedance, as seen at the filter's terminals.

1 Transfer function $\boldsymbol{H}(f)$ analysis

Application of the nodal analysis at the node ① in Fig. 1 directly yields

$$\frac{\boldsymbol{V}-\boldsymbol{V}_\text{i}}{1/\text{j}\omega C_1}+\frac{\boldsymbol{V}}{R_1}+\frac{\boldsymbol{V}-\boldsymbol{V}_\text{o}}{R_2}=0 \Longrightarrow \text{j}\omega C_1\left(\boldsymbol{V}-\boldsymbol{V}_\text{i}\right)+\frac{\boldsymbol{V}}{R_1}+\frac{\boldsymbol{V}-\boldsymbol{V}_\text{o}}{R_2}=0 \tag{1}$$

in which $\boldsymbol{V}$ is the voltage at ① and $\omega = 2\pi f$. The filter must be designed for a pass-band $[f_1, f_2]$, with $f_1 < f_2$ being the lower and upper cutoff frequencies, respectively. By now accounting for the expressions of the relevant cutoff frequencies

$$f_1 = 1/\left(2\pi R_1 C_1\right) \tag{2}$$

$$f_2 = 1/\left(2\pi R_2 C_2\right) \tag{3}$$

Eq. (1) entails

$$\begin{aligned} &\mathrm{j}\,(f/f_1)\,R_2\,(\boldsymbol{V}-\boldsymbol{V}_\mathrm{i})+R_2\boldsymbol{V}+R_1\,(\boldsymbol{V}-\boldsymbol{V}_\mathrm{o})=0 \Longrightarrow \\ &\boldsymbol{V}\,[\mathrm{j}\,(f/f_1)+1+\kappa_R]-\mathrm{j}\,(f/f_1)\,\boldsymbol{V}_\mathrm{i}-\kappa_R\boldsymbol{V}_\mathrm{o}=0 \end{aligned} \tag{4}$$

in which $\kappa_R = R_1/R_2$. Application of the nodal analysis at the node (2) in Fig. 1 yields

$$\frac{\boldsymbol{V}_\mathrm{o}}{1/\mathrm{j}\omega C_1}+\frac{\boldsymbol{V}_\mathrm{o}-\boldsymbol{V}}{R_2}=0 \tag{5}$$

that, upon following similar steps, results into

$$\boldsymbol{V}=\boldsymbol{V}_\mathrm{o}\,[1+\mathrm{j}\,(f/f_2)]\,. \tag{6}$$

Substitution of (6) in (4) yields

$$\boldsymbol{H}(f)=\frac{\boldsymbol{V}_\mathrm{o}}{\boldsymbol{V}_\mathrm{i}}=\frac{\mathrm{j}\,(f/f_1)}{(1-f^2/f_1f_2)+\mathrm{j}\,[f/f_1+f/f_2\,(1+\kappa_R)]} \tag{7}$$

that is the thought for expression of the transfer function. Upon now focusing on the magnitude of the transfer function, (7) directly yields

$$\begin{aligned} |\boldsymbol{H}(f)| &= \frac{f/f_1}{\left\{(1-f^2/f_1f_2)^2+[f/f_1+f/f_2\,(1+\kappa_R)]^2\right\}^{\frac{1}{2}}} \\ &= \frac{1}{\left\{(f_1/f-f/f_2)^2+[1+\kappa_f\,(1+\kappa_R)]^2\right\}^{\frac{1}{2}}} \end{aligned} \tag{8}$$

in which $\kappa_f = f_1/f_2$. Note that, in view of (2) and (3), $\kappa_R = \kappa_C/\kappa_f$, with $\kappa_C = C_2/C_1$ – *mind the reversed definition*. By accounting for this relation in (8) it is found that

$$|\boldsymbol{H}(f)|=\frac{1}{\left[(f_1/f-f/f_2)^2+(1+\kappa_f+\kappa_C)^2\right]^{\frac{1}{2}}} \tag{9}$$

An interesting case arises when $\kappa_R \downarrow 0$ (when $R_2 \gg R_1$), in which case (8) becomes

$$|\boldsymbol{H}_0(f)|=\frac{1}{\left[(f_1/f-f/f_2)^2+(1+\kappa_f)^2\right]^{\frac{1}{2}}} \tag{10}$$

this expression being maximised when $f_1/f-f/f_2=0$ and, thus, for $f_\mathrm{min}=(f_1f_2)^{\frac{1}{2}}$ (the geometrical average of the pass-band's endpoints, as expected), that maximum being

$$|\boldsymbol{H}_0(f)|_\mathrm{max}=|\boldsymbol{H}_0(f_\mathrm{min})|=\frac{1}{1+\kappa_f}. \tag{11}$$

In general, $\kappa_f \approx 0$ (in the case of the EPO-1 power amplifier $\kappa_f = 20/40000 = 5{\cdot}10^{-4}$), implying that $|\boldsymbol{H}_0(f)|$ is, practically, 1 in the pass-band, which is the assumption that is standardly made in EPO-1.

However, as soon as κ_R increases, which can be easily the case in EPO-1 where R_1 is relatively high (47 kΩ), the maximum value of $|\boldsymbol{H}(f)|$ in (8) will (significantly) drop. As clearly inferable from (9), $|\boldsymbol{H}(f)|$ is maximised for the same frequency $f_\mathrm{min}=\sqrt{f_1f_2}$ that will yield a maximum transfer of

$$|\boldsymbol{H}(f)|_\mathrm{max}=|\boldsymbol{H}(f_\mathrm{min})|=\frac{1}{1+\kappa_f+\kappa_C}\approx\frac{1}{1+\kappa_C}. \tag{12}$$

This expression gives a direct indication on the drop in the amplitude of the signal applied to the opamp in the circuit.

To illustrate the effect of the choice for R_1 on $|\boldsymbol{H}(f)|$, a Matlab® parameter study was effectuated with the component and frequency values applying to EPO-1 [1]. In that case, as stated above, $f_1 = 20\,\text{Hz}$ and $f_2 = 40\,\text{kHz}$, entailing a $\kappa_f = 5{\cdot}10^{-4}$, and $R_1 = 47\,\text{k}\Omega$. A number of representative plots are given in Fig. 2. These plots show that a correction of the opamp circuit amplification will be needed (at least) in the cases when R_2 is 1kΩ or lower.

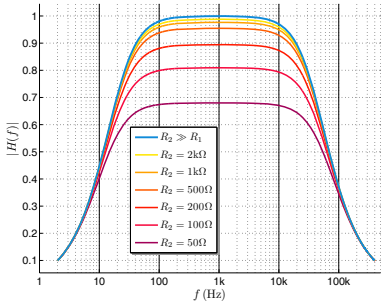

Figure 2: Parameter study of the behaviour of the analysed bandpass filter. The situation when $R_2 \gg R_1$ ($\kappa_R \downarrow 0$) is taken as a reference.

2 Input impedance $\boldsymbol{Z}(f)$ analysis

The second aspect of concern is the frequency dependence of the input impedance $\boldsymbol{Z}(f)$, as seen at the filter's terminals (the left terminals in Fig. 1). Upon assuming that the filter is loaded with a very large, real impedance (a reasonable assumption in view of the opamp's input impedance being in the range of 200 kΩ), the thought for impedance is

$$\boldsymbol{Z}_{\text{in}}(f) = R_1 \left[\frac{1 - \text{j}\,(f_1/f) + \text{j}\,(f/f_2) + \text{j}\kappa_f\,(\kappa_R + 1)}{1 + \text{j}\,(f/f_2)\,(\kappa_R + 1)} \right] \tag{13}$$

In the case when $\kappa_R \downarrow 0$, (13) becomes

$$\boldsymbol{Z}_{\text{in}}(f) = R_1 \left[1 - \text{j}\,\frac{(f_1/f) - \kappa_f}{1 + \text{j}\,(f/f_2)} \right] \tag{14}$$

that is what one should expect in the case of the unloaded high-pass filter consisting of C_1 and R_1 ($\lim\limits_{f\downarrow 0} \boldsymbol{Z}_{\text{in}}(f) = -\text{j}\infty$ and $\lim\limits_{f\to\infty} \boldsymbol{Z}_{\text{in}}(f) = R$). However, as soon as κ_R becomes significant, the frequency behaviour of the input impedance will deviate from this. Upon accounting for the facts that $\kappa_f \kappa_R = \kappa_C$ and $\kappa_f \approx 0$, (13) transforms as

$$\boldsymbol{Z}_{\text{in}}(f) \approx R_1 \left[\frac{1 - \text{j}\,(f_1/f) + \text{j}\,(f/f_2) + \text{j}\kappa_C}{1 + \text{j}\,(f/f_1)\,\kappa_C + \text{j}\,(f/f_2)} \right] = R_1 \left[1 - \text{j}\,\frac{(f_1/f) + (f/f_1)\,\kappa_C - \kappa_C}{1 + \text{j}\,(f/f_1)\,\kappa_C + \text{j}\,(f/f_2)} \right]. \tag{15}$$

For $f \downarrow 0$ (15) will still yield the expected $-\text{j}\infty$ value. However

$$\lim_{f\to\infty} \boldsymbol{Z}_{\text{in}}(f) \approx R_1 \left[1 - \text{j}\,\frac{\kappa_C}{\kappa_C + \kappa_f} \right] \approx R_1(1 - \text{j}). \tag{16}$$

All these formulas show that the lower limit of the input impedance seen at the power amplifier's terminals is determined by R_1, that justifies the choice for its large resistance.

References

[1] G. J. M. Janssen, J. F. Creemer, D. Djairam, M. Gibescu, I. E. Lager, N. P. van der Meijs, S. Vollebregt, B. Roodenburg, J. Hoekstra, S. Izadkhast, and X. van Rijnsoever, *Lab Courses EE Semester 1. Student Manual. Year 2019-2020*, Delft, the Netherlands: Delft University Of Technology, 2019.